Helium burning and neutron sources in the stars

EPJ A
Hadrons and Nuclei

EPJ.org
your physics journal

Eur. Phys. J. A (2016) **52**: 76 DOI 10.1140/epja/i2016-16076-3

Helium burning and neutron sources in the stars

M. Aliotta, M. Junker, P. Prati, O. Straniero and F. Strieder

Società Italiana di Fisica

Springer

Eur. Phys. J. A (2016) **52**: 76
DOI 10.1140/epja/i2016-16076-3

THE EUROPEAN PHYSICAL JOURNAL A

Regular Article – Experimental Physics

Helium burning and neutron sources in the stars*

M. Aliotta[1], M. Junker[2], P. Prati[3,a], O. Straniero[4], and F. Strieder[5]

[1] SUPA, School of Physics and Astronomy, University of Edinburgh, Edinburgh, UK
[2] Laboratori Nazionali del Gran Sasso (LNGS), Assergi, Italy
[3] Università degli Studi di Genova and INFN, Sezione di Genova, Genova, Italy
[4] Osservatorio Astronomico di Collurania, Teramo, Italy
[5] South Dakota School of Mines and Technology, Rapid City, SD 57701, USA

Received: 31 July 2015 / Revised: 27 November 2015
Published online: 5 April 2016 –
Communicated by C. Broggini

Abstract. Helium burning represents an important stage of stellar evolution as it contributes to the synthesis of key elements such as carbon, through the triple-α process, and oxygen, through the $^{12}C(\alpha,\gamma)^{16}O$ reaction. It is the ratio of carbon to oxygen at the end of the helium burning stage that governs the following phases of stellar evolution leading to different scenarios depending on the initial stellar mass. In addition, helium burning in Asymptotic Giant Branch stars, provides the two main sources of neutrons, namely the $^{13}C(\alpha,n)^{16}O$ and the $^{22}Ne(\alpha,n)^{25}Mg$, for the synthesis of about half of all elements heavier than iron through the s-process. Given the importance of these reactions, much experimental work has been devoted to the study of their reaction rates over the last few decades. However, large uncertainties still remain at the energies of astrophysical interest which greatly limit the accuracy of stellar models predictions. Here, we review the current status on the latest experimental efforts and show how measurements of these important reaction cross sections can be significantly improved at next-generation deep underground laboratories.

1 Introduction

Helium burning represents a fundamental step in the chemical evolution of the Universe as it contributes to the synthesis of carbon, a key building block of any known form of life. No carbon was synthesised during the primordial nucleosynthesis that followed the Big Bang, essentially because of the lack of stable nuclei with mass $A = 5$ and 8. However, at the time of the Solar System formation, some 8 Gyr after the Big Bang, about 0.3% of the total baryonic matter was made of carbon, indicating that carbon could be forged in stars. It was Fred Hoyle, in the 1950s, to suggest that such a stellar C production was possible thanks to a state in the ^{12}C nucleus at ~ 7.7 MeV [1] that allowed for a resonant fusion of three alpha particles during helium burning in stars. Without this resonance, the triple-α reaction would not be fast enough to account for the amount of carbon observed in the Universe and life, as we know it, could not exist.

Carbon, however, is not the only important product of He burning. Indeed, oxygen is likely the most abundant yield, through the $^{12}C(\alpha,\gamma)^{16}O$ reaction, while the synthesis of heavier elements by further alpha-particle captures is hindered by the increased Coulomb barrier and the comparatively low thermal energies characteristic of hydrostatic He burning.

Thus, carbon and oxygen represent the main nucleosynthesis products of stellar helium burning and their relative abundance at the end of the He-burning phase, the C/O ratio, greatly affects a star's subsequent evolution. For instance, low- and intermediate-mass stars terminate their lives as C-O White Dwarfs (WD), with cooling time scales determined by the C/O ratio: the larger the C/O ratio the faster the cooling (see, for example [2]). By contrast, massive stars will proceed through a stage of C burning, later followed by Ne-, O- and Si-burning stages ending with the formation of iron in the stellar core. As further nuclear fusions become endothermic, the star subdues to the gravitational force, its core collapses into highly neutronised matter, and the envelope bounces off leading to an outward shockwave that disrupts the star. Such an event is known as a core-collapse supernova explosion, with type-IIp supernovae (SNe) being the most common type [3]. Once again, observational features of these events, such as their light curves and the chemical composition of their debris, are largely determined by the C/O ratio left after the He-burning epoch [4].

* Contribution to the Topical Issue "Underground nuclear astrophysics and solar neutrinos: Impact on astrophysics, solar and neutrino physic" edited by Gianpaolo Bellini, Carlo Broggini, Alessandra Guglielmetti.

[a] e-mail: prati@ge.infn.it

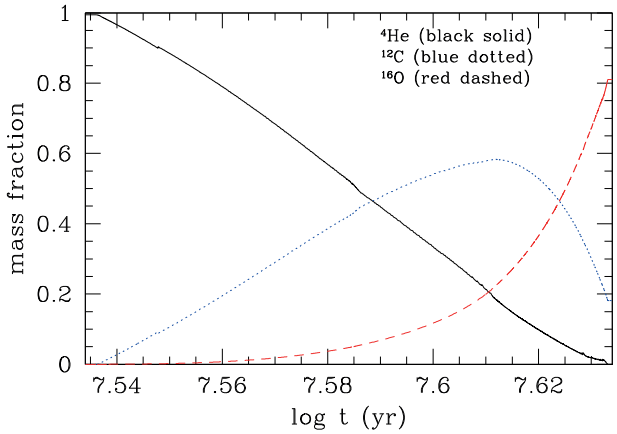

Fig. 1. Temporal evolution of the central values of the He, C and O mass fractions in a stellar model with $M = 7M_{\odot}$. At the beginning of the core He-burning phase, the dominant process is the triple-α that produces ^{12}C. Later on, the onset of the $^{12}\mathrm{C}(\alpha,\gamma)^{16}\mathrm{O}$ reaction allows for a substantial oxygen production. The final C/O ratio depends on the adopted reaction rates for both processes. For this model, reaction rates from NACRE [6] and Kunz *et al.* [7] have been used for the triple-α and the $^{12}\mathrm{C}(\alpha,\gamma)^{16}\mathrm{O}$, respectively.

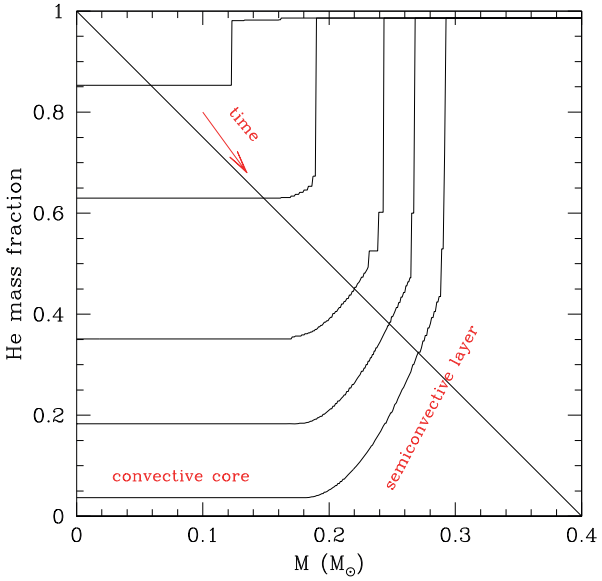

Fig. 2. Time evolution of the He mass fraction in the core of a $3M_{\odot}$ model during the core-He-burning phase. As He is consumed (and transformed into C and O) the fully convective core grows in mass, while an external semi-convective layer develops. The interplay between convective mixing and nuclear burning determines important features of later evolution, such as the time scale and chemical yields (see [4]).

Likewise, the explosive features of a different class of supernovae events, type Ia, largely used in observational cosmology as distance indicators for high redshift galaxies, are also affected by the C/O ratio in the core prior to the thermonuclear runaway that powers the explosion [5].

In stars with mass larger than $2M_{\odot}$, He burns quiescently in the core at temperatures $T = 100$–200 MK, corresponding to Gamow peak energies $E_0 \sim 200$–300 keV for both the triple alpha and the $^{12}\mathrm{C} + \alpha$ reactions. Clearly, the amounts of C and O produced in the core depend on the relative rate of both processes. Figure 1 shows the evolution of the central abundances of He, C and O for a $7M_{\odot}$ star model, as an example. Initially, the triple-α reaction dominates the burning process. Later on, when a sufficient amount of C has been accumulated, the production of O begins.

In low-mass stars, He burning proceeds like in more massive objects, except for a short thermonuclear runaway (He flash) that occurs under electron degeneracy conditions in the high-density core. However, once the temperature increases following the He flash, the degeneracy is removed and quiescent He burning settles in.

The interplay between convection and nuclear burning plays a fundamental role in the advanced phases of stellar evolution. A convective instability arises when the temperature gradient exceeds a critical value. In most cases this critical value coincides with the adiabatic temperature gradient (Schwarzschild criterion). On the other hand, the temperature gradient depends on the power of the energy source (or its luminosity) and on the energy transfer mechanism. For instance, in the case of radiative transfer, it is

$$\nabla_{\mathrm{rad}} = \frac{3\kappa r^2 P}{4acGM_r T^4} F = \frac{3\kappa r^2 P}{4acGM_r T^4} \frac{L_r}{4\pi r^2}\,, \qquad (1)$$

where

$$\nabla = \frac{\mathrm{d}\ln T}{\mathrm{d}\ln P}\,, \qquad (2)$$

F is the energy flux, L the luminosity, M the mass, P the pressure, T the temperature, κ is the radiative opacity, G is the gravitational constant, c is the speed of light and a the radiation pressure constant. All quantities are computed at the radius r (spherical symmetry is here assumed for simplicity). At the onset of the He burning, the energy flux generated by the triple-α reactions induces the formation of a convective core. As He is converted into C and O, the radiative opacity increases and the convective core progressively grows in mass. Eventually, a semi-convective layer appears outside the convective core, where a partial mixing regulates the $\mathrm{He/C+O}$ ratio in such a way that convective neutrality is attained [8]. The evolution of the He profile during core He burning is shown in fig. 2, for the innermost fraction ($M/M_{\odot} < 0.4$) of the stellar core. At the beginning of core He burning, the He profile is flat (~ 1 everywhere in the core). As the burning proceeds, He is consumed near the centre and its depletion propagates outwards through convection. The stepped profiles (second and third curves starting from the top) illustrate this occurrence. The extension of the convective core increases with time. At a certain time, a semi-convective layer develops just outside the fully convective core.

After all helium has been exhausted in the stellar core, He burning proceeds just outside the newly formed C-O core. In low- and intermediate-mass stars, this occurrence marks the beginning of the Asymptotic Giant Branch (AGB) phase, during which the two burning shells

(H and He) become alternatively active. After an initial quiescent phase (early AGB), the He-burning shell gets progressively closer to the outer border of the H-exhausted core and, eventually, He burning dies down. Then, fresh He produced by the H shell burning accumulates around of the C-O core, until a critical mass is attained and He ignites at the base of an He-rich buffer. A thermonuclear runaway follows (called thermal pulse), during which temperatures as high as $3–4 \times 10^8$ K are attained. It is during this stage that two other important He-burning reactions take place, namely, the $^{13}C(\alpha, n)^{16}O$ and the $^{22}Ne(\alpha, n)^{25}Mg$ (for a recent review see [9]). Both reactions provide the key neutron sources for the synthesis of elements heavier than iron. The first is active during the interpulse phase, when the H burning is on and the He burning is off. Its main feature is the low neutron density ($\sim 10^7$ neutrons/cm^3), sustained for rather long timescales (10^5 yr in low-mass AGB stars). The second is active at the base of the convective zone generated by the thermal pulse and it is characterised by a higher neutron density (up to 10^{13} neutrons/cm^3 in massive AGB stars). The $^{13}C(\alpha, n)^{16}O$, in particular, is responsible for the production of the cosmic abundances of the so-called main and strong components of the s-process (about half of the stable isotopes with mass $A \geq 90$) [10]. The $^{22}Ne(\alpha, n)^{25}Mg$ reaction may be activated also during the core-He burning of massive stars. In this case a moderate neutron exposure may induce the production of the so-called weak component of the s-process ($60 \leq A \leq 90$) [11].

Finally, He burning can also occur explosively in close binary systems harbouring compact White Dwarfs with sub-Chandrasekhar mass. The most interesting case is that of the He detonation supernova, a model proposed to explain some peculiar (sub-luminous) type-Ia SNe; they are the result of He accretion on a C-O WD from a He star [12]. In case of a stationary accretion, a He-rich layer accumulates on the WD until a critical mass is attained and a He detonation occurs, followed by a delayed C detonation (for this reason such events are also classed as double-detonation SNe). In the He-burning zone, peak temperatures of several GK are attained. By the end of the explosion, all the original He-rich accreted material is converted into iron peak isotopes [13].

Given the importance of the three main He-burning reactions mentioned, it is not surprising that much experimental effort has been devoted to the direct measurement of their cross sections and impressive progress has been attained so far. However, the precision achieved is still far from that required by stellar models.

In this paper, we review the current status of recent measurements and show how further improvements can be obtained at a deep underground laboratory such as LUNA.

2 Review of the state of the art

2.1 The reaction $^{12}C(\alpha, \gamma)^{16}O$

In the early stages of He burning, the only active process is the triple-α reaction, because the ^{12}C abundance is still too low. After a significant abundance of carbon has been built up, the $^{12}C(\alpha, \gamma)^{16}O$ reaction becomes the dominant process. Its cross section at the relevant Gamow energy, $E_0 \simeq 300$ keV, determines the helium burning time scale and, together with the convection mechanism, the abundances of carbon and oxygen at the end of helium burning. However, large uncertainties in the efficiency of convection-induced mixing complicate predictions of the central oxygen mass fraction [8, 14]. Thus, an experimental determination of the $^{12}C(\alpha, \gamma)^{16}O$ cross section in the relevant energy region with a precision of 10% or better is needed to improve our knowledge of the convection processes and remains an important ingredient for the understanding of stellar evolution.

The cross section of the reaction $^{12}C(\alpha, \gamma)^{16}O$ ($Q = 7.162$ MeV) is dominated by $E1$ and $E2$ capture processes into the ^{16}O ground state, where the two multipoles appear to be of similar importance. At the He-burning Gamow energy, the total reaction cross section is of the order of 10^{-17} b, by far too small for direct measurements with present and future experimental capabilities. As a consequence, an extrapolation into the relevant energy range is mandatory. The $E1$ amplitude arises from the low-energy tail of a broad $J^\pi = 1^-$ resonance at $E_R = 2.42$ MeV ($\Gamma_R = 400$ keV), the high-energy tail of a $J^\pi = 1^-$ sub-threshold resonance at $E_R = -45$ keV, and the low-energy tail of an unidentified background amplitude due to broad $J^\pi = 1^-$ resonances at high energies; interference effects between these $E1$ sources must also be included. The $E2$ amplitude arises predominantly from the high-energy tail of a $J^\pi = 2^+$ sub-threshold resonance at $E_R = -245$ keV, the $E2$ direct capture process, and the low-energy tails of broad $J^\pi = 2^+$ resonances at high energies. Since the capture cross sections of the $E1$ and $E2$ multipoles have different energy dependencies, one must have an independent and precise information on the energy dependence of each multipole cross section for an extrapolation to E_0.

In addition to the ground state contributions, cascade transitions have to be considered whereas much fewer data are available. The cascade transitions can proceed through a number of ^{16}O excited states and in particular transitions to the $E_x = 6.92$ MeV ($J^\pi = 2^+$) and 7.12 MeV ($J^\pi = 1^-$) have been observed.

Several direct γ-ray spectroscopy experiments [7, 15–28] were carried out over the last almost 50 years to measure the $^{12}C(\alpha, \gamma)^{16}O$ cross section. Additional information can be derived from measurements of the (α, α)-elastic scattering [29–32], the β-delayed α-decay of ^{16}N [33–36], transfer reactions [37–39], and the total cross section with a recoil separator [40].

Currently, about ten data sets exist on the $^{12}C(\alpha, \gamma)^{16}O$ $E1$ and $E2$ ground-state transitions covering an overall (presumably not all data sets cover the same region) energy region $E = 0.9$ to 3.3 MeV and, more recently, one measurement at even higher energies [27]. These data differ in their statistical precision but also disagree in the absolute normalization. The latter issue hampers a combined fit of all data sets. Older experiments often lack details on

the analysis procedure and uncertainty determination, in particular statistical and systematic uncertainties are not properly disentangled. Furthermore, some measurements, *e.g.* [16, 17, 21], were performed with low-resolution scintillator detectors in close geometry. Thus, the analysis of the γ-ray spectra is extremely sensitive to the background treatment and probably led to an underestimation of the uncertainty.

In the analysis of the angular distributions, the relative phase was often used as a fit parameter [18, 20, 24] resulting in a large scattering of these values inconsistent with the results from elastic scattering. Note that the relative phase in principle can be calculated from the $l = 1$ and 2 phase shift data. This lack of internal consistency in some works was already noted in previous R-matrix evaluations, *e.g.* by Brune [41], and represents an ambiguity in these angular distribution analyses.

The importance of the $J^\pi = 0^+$ state at $E_x = 6.05$ MeV in ^{16}O was emphasized in a work by Matei *et al.* [25]. An excited 0^+ state decays exclusively by an $E0$ e^+e^- transition to the 0^+ ground state and only the primary γ-ray line can be observed. This component was measured with the DRAGON recoil separator at TRIUMF, Canada, in the energy region $E = 2.22$ to 5.42 MeV with a high efficiency BGO array in coincidence with the observed recoils. The data have been analyzed with an R-matrix calculation and extrapolated to the astrophysical energy region, $S_{6.05}(300) = 25^{+16}_{-15}$ keV b. However, this analysis has been recently questioned by a direct γ-ray measurement of this transition at higher energies [27] and a determination of the asymptotic normalization coefficient (ANC) of the corresponding state in ^{16}O [39]. Both studies suggest that the contribution of cascade transitions to the total S factor is small.

The extrapolation of the astrophysical S factor is usually described in the R-matrix formalism (see [41–43] for details). The corresponding fit should include all available information from direct as well as indirect studies and properly take into account the different systematic uncertainties of the various experiments. Higher-energy direct data can often constrain interference pattern in the individual multipole fits which are not sufficiently determined by low-energy γ-ray measurements. Such an extended analysis was performed by Schürmann *et al.* [44] leading to an extrapolation at astrophysical energies of $S(300) = 161 \pm 19_{\rm stat}{}^{+8}_{-2}$sys keV b where the uncertainty was determined using a Monte Carlo approach as in [22]. However, in a recent work [45] the quality of the published low-energy γ-ray angular distribution data was heavily questioned and the ambiguity arising from the choice of the $E1$ interference pattern between the broad 1^- resonance at $E_R = 2.42$ MeV and the 1^- subthreshold resonance was underlined. The current low-energy data strongly support a constructive interference as assumed in [44] and most other previous analyses, but a destructive interference would reduce the total S factor by almost a factor of 2 compared to the result of [44].

A new dedicated direct γ-ray measurement of the ^{12}C$(\alpha,\gamma)^{16}$O cross section with an increased sensitivity would certainly help to solve this remaining ambiguity and reduce the uncertainty in the reaction rate at astrophysical temperatures to a level that stellar models can deliver significantly improved predictions. Currently, low-energy measurements of the ^{12}C$(\alpha,\gamma)^{16}$O reaction in Earth's surface laboratories are not only limited by low yields, but also by beam-induced background from the ^{13}C$(\alpha,n)^{16}$O reaction arising from ^{13}C contaminants in ^{12}C targets. As a matter of fact, this major source of background is almost unavoidable during target production via ^{12}C implantation. However, additional mass separation during the implantation process or new target production techniques might further improve the ^{12}C/^{13}C ratio compared to previous works. Alternatively, an experiment in inverse kinematics with an intense ^{12}C beam and a ^{4}He jet gas target in conjunction with a high-granularity, high-efficiency γ-ray detector array might be an even better experimental approach for the future since in this configuration the limiting background contribution is given by cosmic-ray background [22].

The γ-ray detection system must fulfil several requirements:

1) High detection efficiency at energies around 7 MeV. Such energy region is particularly difficult because the γ-ray interaction cross-section has a minimum there. The main source of background are the γ-rays emitted from neutron-capture reactions occurring in the materials around the detector. These γ-rays have typically energy in the range 10–15 MeV. Therefore, the detector should have a high efficiency in the reconstruction of the total γ-ray energy, in order to enhance the signal-to-background ratio.
2) Good energy resolution to separate signal from background even with a poor statistics of events.
3) Segmentation along the θ angle in order to measure the angular distribution.
4) Segmentation in both angles θ and ϕ to detect the radiative cascades.
5) Large solid angle, close to 100%.

The need of high efficiency and good energy resolution at 7 MeV points towards scintillating crystals with high density and high atomic numbers.

2.2 The ^{13}C$(\alpha,n)^{16}$O

Neutron capture nucleosynthesis can occur in low-mass AGB stars via the s-process [46]. This process can account for the production of about half of the stable isotopes beyond iron in the universe. The neutrons needed to fuel the process are produced by the ^{13}C$(\alpha,n)^{16}$O reaction. With relevant astrophysical temperatures between 90 and 100 MK the Gamow window for this reaction is located between 180 and 200 keV.

In AGB stars, a radiative zone enriched in ^{13}C, called the ^{13}C pocket, forms within a helium-rich mantel as a consequence of the third dredge up [46]. During the interpulse, *i.e.* the period between two subsequent thermal pulses, this zone contracts and heats up, until the

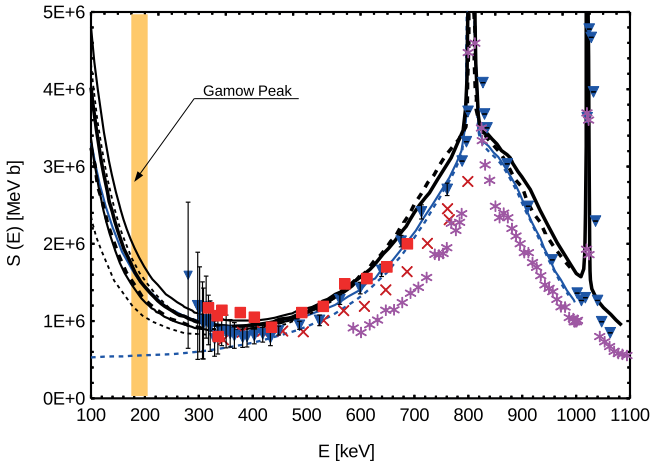

Fig. 3. S factor data obtained in most recent direct experiments. Squares (red): Heil *et al.* [47], triangles (blue): Drotleff *et al.* [50], crosses (red): Brune *et al.* [51], stars (magenta): Harrissopolus *et al.* [53]. In addition the extrapolations by Pellegriti *et al.* [58] (continuous black line) and La Cognata *et al.* [61] (dashed black line) are shown together with the respective uncertainty band. The upper (lower) blue line represents the data fit by Heil *et al.* [47] including (not including) the contribution from the 6.356 MeV, $J^\pi = 1/2^+$ state in ^{17}O.

^{13}C$(\alpha, n)^{16}$O reaction starts to release neutrons which feed the s-process.

In the most metal-rich stellar models with an almost solar composition, a small amount of ^{13}C might survive and be engulfed into the convective zone generated by the incoming thermal pulse. In this scenario, the ^{13}C$(\alpha, n)^{16}$O reaction occurs at relatively high temperatures resulting in a neutron density of 10^{11} neutrons/cm^3, to be compared with 10^7 neutrons/cm^3 produced during radiative ^{13}C burning. The amount of unburned ^{13}C left at the end of the interpulse and available to produce neutrons in the subsequent pulse depends on the rate of the ^{13}C$(\alpha, n)^{16}$O reaction. Using the current rate by Heil *et al.* [47], all the ^{13}C is consumed before the interpulse ends.

The scenario would affect several branching points along the s-process path. Large excesses of ^{60}Fe, ^{86}Kr, ^{87}Rb or ^{96}Zr are expected compared to the radiative (low neutron density) ^{13}C burst [46, 48, 49].

The ^{13}C$(\alpha, n)^{16}$O reaction ($Q = 2.216$ MeV) has been studied over a wide energy range by direct measurements. Neutrons have been detected either with ^{3}He gas counters [50–53] or with a high-efficieny BaF_2 array after the neutrons were transformed into γ rays through the reaction ^{113}Cd$(n, \gamma)^{114}$Cd reaction [47].

The results of some of these experiments are summarized in fig. 3. While the slope of the different data sets is consistent, the results show a large scatter in absolute normalization. Furthermore, none of the available data set reaches the Gamow window and thus extrapolations are mandatory. To achieve this goal, Heil *et al.* performed a multichannel R-matrix study including the reactions: ^{16}O$(n, n)^{16}$O, ^{16}O$(n, n'\gamma)^{16}$O, ^{13}C$(\alpha, \alpha)^{13}$C and ^{16}O$(n, \alpha)^{13}$C. Owing to a large systematic discrepancy, attributed to problems in the efficiency calibration of the detector, the data of [53] have not been considered while the other data sets were normalized by empirically determined scaling factors [47].

Table 1. Summary of the S_α and the $\tilde{C}^2$ values for the $1/2^+$ sub-threshold state obtained via transfer reactions [55–60] and via the Trojan Horse Method [61]. The data set of [56] was reanalyzed in [57] (see [57] for details). Experimental problems in the data by [59] were identified in [60] (see text for details).

Method	S_α	$\tilde{C}^2$ [fm^{-1}]	Reference
^{13}C$(^6$Li, $d)^{17}$O	0.011		[56]
^{13}C$(^7$Li, $t)^{17}$O	0.29 ± 0.11	4.5 ± 2.2	[58]
^{13}C$(^6$Li, $d)^{17}$O	0.15 to 0.41		[57]
^{13}C$(^{11}$B, ^{7}Li$)^{17}$O	0.37 ± 0.12	4.0 ± 1.1	[55]
^{6}Li$(^{13}$C, $d)^{17}$O		0.89 ± 0.23	[59]
^{6}Li$(^{13}$C, $d)^{17}$O		3.6 ± 0.7	[60]
^{13}C$(^6$Li, n^{16}O$)d$		$6.7^{+0.9}_{-0.6}$	[61]

The work of Heil *et al.* confirms the finding of Descouvemont with a microscopic model, the generator-coordinate method (GCM) [54]: At energies inside the Gamow window, the S factor strongly depends on the α-width Γ_α of the 6.356 MeV, $J^\pi = 1/2^+$ state in ^{17}O. Γ_α can be derived either from the spectroscopic factor S_α or from the asymptotic normalization coefficient (ANC) $\tilde{C}^2$ [55]. In oder to reduce the uncertainty of the extrapolation, S_α and $\tilde{C}^2$ of the 6.356 MeV, $J^\pi = 1/2^+$ state have been determined experimentally exploring transfer reactions [55–60] as well as the Trojan Horse Method (THM) [61]. The results of these measurements are summarized in table 1.

The S_α of 0.011 obtained in [56] appears to be an order of magnitude lower than those published by [55, 58] resulting in a negligible contribution of the 6.356 MeV, $J^\pi = 1/2^+$ state in ^{17}O. Keeley *et al.* [57] re-analyzed the data of [56] and published a revised S_α value between 0.15 and 0.41.

The values of $\tilde{C}^2$ published in [55, 58, 60] are in good agreement while the value published in Johnson *et al.* [59] is about a factor of four lower. As Avila *et al.* [60], Johnson *et al.* exploited sub-Coulomb α-transfer reaction ^{6}Li$(^{13}$C, $d)^{17}$O. Avila *et al.* observed that the use of ^{13}C beam causes the build up of a dead layer on the ^{6}Li target when targets are not changed frequently. This dead layer reduces the energy of the ^{13}C ions before they reach the active ^{6}Li material. Because of the exponential energy dependence of the cross section at energies below the Coulomb barrier, the reduced interaction energy results in a significantly lower cross section. While Avila *et al.* addressed this problem by frequent changes of target, the effect has not been considered by Johnson *et al.* [60]. The measurements [55, 58] are less sensitive to this effect due to the use of ^{7}Li and ^{11}B beams, respectively. The discrepancy between the different results obtained by α transfer reactions is thus removed [60].

A renewed determination of $\tilde{C}^2$ exploiting the Trojan Horse Method (THM) [61] claims a higher accuracy and reliability compared to other indirect techniques. Even though this $\tilde{C}^2$ value is significantly higher than the values published by [55, 58, 60], all of them support the hypothesis of a significant contribution of the -3 keV resonance to the total low-energy cross section.

In conclusion, recent indirect investigations indicate a significant impact of -3 keV sub-threshold resonance on the astrophysical S factor of the $^{13}C(\alpha, n)^{16}O$ reaction inside the Gamow peak.

Several authors performed extrapolations of the S factor using the Breit-Wigner formalism [55, 56] or the R-matrix method [47, 58, 61]. Figure 3 displays the fits published by [47, 55, 61] together with the original data set obtained by [47, 50, 51, 53]. Within the Gamow window, the S factor extrapolation appears to be dominated by the impact of the 6.356 MeV, $J^\pi = 1/2^+$ state in ^{17}O which contributes $\approx 70\%$ of the S factor at $E = 190$ keV [58]. There remains, however, an uncertainty on the extrapolated S factor of $\approx 40\%$ at $E = 190$ keV. Uncertainties related to the absolute normalization of the data are not taken into account in this value; thus, it may be largely underestimated.

In order to significantly improve upon the present situation, new direct measurements are desirable. Because of the low cross section, direct measurements, inside the Gamow window, with statistical uncertainties of less the than 10% remain out of reach with the available accelerator and detection systems: extrapolations remain unavoidable. Consequently, a renewed direct study of the reaction should be designed to support the mandatory extrapolation by covering a wide energy range from several MeV down to a few hundreds of keV, featuring at the same time small statistical uncertainties of not more than 10% even at the lowest energies. This precision would allow to directly constrain the impact of the 6.356 MeV, $J^\pi = 1/2^+$ state in ^{17}O. Furthermore, because of the uncertainties in the absolute scale of the data, normalization procedures must be carefully taken into consideration.

2.3 The $^{22}Ne(\alpha, n)^{25}Mg$

The $^{22}Ne(\alpha, n)^{25}Mg$ reaction is the main neutron source for the s-process in core He-burning massive stars ($M > 8M_\odot$) and in He-shell burning AGB stars. For this reason, it has been extensively studied since 1969 (see [62] and references therein). The Q-value is negative and when approaching the reaction threshold ($E_\alpha = 560$ keV), the small values of both the cross section and the kinetic energy of the emitted neutrons make the direct measurement extremely challenging. As a matter of fact, the current status of the available data at energies of astrophysical interest ($E_\alpha = 0.56$–10 MeV) is far from a satisfactory level of accuracy, in particular for $E_\alpha < 1$ MeV. Here, we focus the discussion on recent progress in both the experimental data and the calculation of the stellar reaction rate.

The last comprehensive experimental study was performed by Jaeger *et al.*, in 2001 [63]. Enriched ^{22}Ne gas

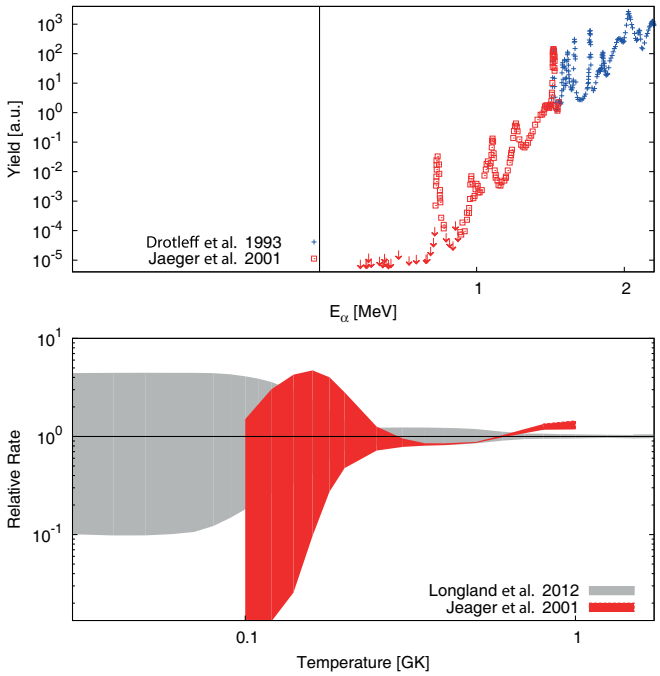

Fig. 4. State of the art for the $^{22}Ne(\alpha, n)^{25}Mg$. Top panel: excitation function at $E_\alpha < 2.3$ MeV. The arrows indicate Jaeger *et al.* [63] upper limits. Bottom panel: reaction rate and uncertainty normalized to the recent calculation of Longland *et al.* [64].

(99.9%) was used and continuously recirculated after purification. The neutron detection was ensured by a 4π system consisting in a cylinder of polyethylene moderator hosting 12 ^{3}He-proportional counters. The total detection efficiency was around 50%. The experiment explored the energy range from the reaction threshold to $E_\alpha = 1.5$ MeV, resulting in a detailed excitation function reproduced in fig. 4, upper panel. Due to the limitation in the luminosity and in the cosmic-ray background reduction, runs at $E_\alpha < 1$ MeV actually resulted in upper limits only, with the significant exception of the resonance at $E_\alpha = 832$ keV, whose strength was determined to be $\omega\gamma = (118 \pm 11)\,\mu$eV [63]. Based on these results, Jaeger *et al.*, calculated the reaction rate as the folding integral between the excitation function and the stellar Maxwell-Boltzmann velocity distribution. In this calculation (see fig. 4, lower panel), they made an important and partially controversial assumption fixing the strength of the hypothetical resonance at $E_\alpha = 635$ keV [65] at 10% of its observed upper limit. The calculated reaction rate, even with an uncertainty significantly reduced with respect to previous works, is still not firm enough at temperatures below $T_9 = 0.3$ K [63].

A refined analysis of all the available data was carried out by Longland *et al.* in 2012 [64]. This new evaluation of the reaction rate is based on three assumptions. First, the existence of the resonance at $E_\alpha = 635$ keV was excluded, based on a previous work [66] which showed that the $E_x = 11154$ keV level of ^{26}Mg has unnatural parity. Second, the resonance strength uncertainty of all available data sets was inflated to account for a systematic

contribution to the error budget by a chi-square minimization procedure. Third, in case resonance strengths are available as upper limits only, these resonances were treated by a quite complex methodology based on a Monte Carlo simulation fed by a truncated Porter-Thomas distribution [67] of the reduced resonance widths. This elaborated data treatment was considered more realistic than that of [68]. The results of Longland *et al.* [66] are here compared (fig. 4, lower panel) with the corresponding calculation by Jaeger *et al.* [63]. Significant uncertainties still remain near the reaction threshold. Given that the current situation heavily depends on the data reduction approach, improved experimental information is critically necessary [68].

Hence, a new direct measurement with a unique set-up in a wide energy range and in conditions of high luminosity and reduced background is desirable with the goal to improve the overall accuracy and further reduce (or even eliminate) the present upper limits. This frame calls for an underground accelerator facility equipped with a gas target and state-of-the-art neutron detectors.

3 Perspectives for next-generation underground experiments

For the $^{12}C(\alpha,\gamma)^{16}O$, $^{13}C(\alpha,n)^{16}O$ and $^{22}Ne(\alpha,n)^{25}Mg$ reactions, characteristic temperatures of helium burning, $T = (0.9\text{–}3) \times 10^8$ K, translate into energies of astrophysical interest of a few hundreds of keV (between $E_{cm} \simeq$ 150–750 keV at most depending on reaction) and thus orders of magnitude lower than the Coulomb barriers between interacting nuclei (about 5 and 7 MeV for the reactions involving ^{12}C and ^{22}Ne, respectively). As a result, the cross sections of interest drop exponentially into the realm of femtobarns or lower and the corresponding experimental yields become increasingly difficult to measure, the lower the interaction energy. A quick back-of-the envelope calculation shows the tremendous challenges facing the experimentalists. For typical stable-nuclei beam currents of a few hundreds of μA (10^{14} pps), solid target densities of 10^{19} atoms/cm^2, and reaction cross sections $\sigma = 10^{-15}$ barn, experimental reaction yields may be as low as 30 counts/year assuming 100% detection efficiency! Clearly, such counting rates demand for extremely long measuring times, controlled and stable experimental conditions, maximum detection efficiencies, and above all minimal background, whether natural or beam induced. Indeed, the signals produced by background events arising from the interaction of cosmic rays with the experimental setup, from natural ambient radioactivity, or from beam-induced reactions remain the most limiting factor to low-energy measurements of nuclear astrophysics reactions.

In some cases, the extrapolation of high-energy data aided by the *R*-matrix formalism is adequate to obtain reaction rates with sufficient precision for astrophysical modelling of stellar evolution and nucleosynthesis. In general, however, reaction-specific uncertainties greatly complicate the analysis of experimental data and lead to largely uncertain astrophysical rates. This is the case, for example, of the complex interplay between $E1$ and $E2$ contributions to the $^{12}C(\alpha,\gamma)^{16}O$ reaction cross section; the possible presence of sub-threshold states in the $^{13}C(\alpha,n)^{16}O$ reaction; or the extreme weakness of potentially important resonances in the $^{22}Ne(\alpha,n)^{25}Mg$ reaction. Often, indirect methods, albeit model-dependent, offer useful complementary approaches to direct measurements. Various techniques [69] have been used over the decades to overcome or at least mitigate key limitations of direct measurements. Each approach has its own set of advantages and disadvantages, but all offer the possibility to cross check for systematic effects which may potentially skew experimental results. By contrast, major advances in direct measurements can now only come from further efforts to minimise background sources, both natural and beam-induced. Underground laboratories provide a unique opportunity to this end, both for γ-ray and neutron detection.

The main source of γ-ray background at energies below $E_\gamma = 3.5$ MeV arises from radionuclides of both cosmogenic (^{3}H, ^{7}Be, ^{14}C, ^{26}Al, ^{60}Co) and artificial origin (^{95}Nb, ^{144}Ce, ^{134,137}Cs), as well as short-lived (^{222}Rn) and long-lived (*e.g.*, ^{40}K, ^{87}Rb, ^{133}La) radionuclides ([70] and references therein). At energies above $E_\gamma = 2.6$ MeV the background is mostly dominated by cosmic-ray (muon and neutron-induced) interactions with the experimental setup. Active and passive shielding as well as γ-γ coincidence techniques (*e.g.*, [71]) can both effectively reduce the background in this energy region. However, their application may be limited to specific reactions and almost invariably lead to reduced detection efficiencies. Far more effective is to perform γ-ray spectroscopy studies in laboratories deep underground. At LUNA, the shielding provided by the 1.4 km of rock overburden above the experimental halls affords a six-order-of-magnitude reduction in cosmic-ray muon background [70, 72], thus also allowing for more effective additional (passive) shielding than can be achieved on a surface laboratory. The advantage of going underground is thus evident for reactions that give rise to high-energy γ-rays, especially when other sources of background (*e.g.*, beam-induced) can also be minimised. Specifically, for the $^{12}C(\alpha,\gamma)^{16}O$ reaction, the beam-induced background is due to (n,γ) events following the $^{13}C(\alpha,n)^{16}O$ reaction between an α-particle beam and ^{13}C impurities in the target. This beam-induced background can be completely eliminated by performing the experiment in inverse kinematics, using a ^{12}C beam instead, as planned at LUNA MV, the new 3.5 MV accelerator facility in construction at LNGS, Italy [73].

The LUNA-MV accelerator is presently being tendered by INFN. It will be an electrostatic single ended machine designed to produce H^+, He^+, $^{12}C^+$ and $^{12}C^{++}$ beams of approximately 500, 300, 100 and 80 μA, respectively. Beam energies for these species will range from 0.3 MeV to 3.5 MeV. As nuclear cross sections drop exponentially at energies below the Coulomb barrier, utmost importance has been given to high reliability of ion beam energy stability and its absolute determination. In order to allow for long expected measurement time, specially at low energies the machine will be designed to allow for operation without operator on site for more than 12 hours.

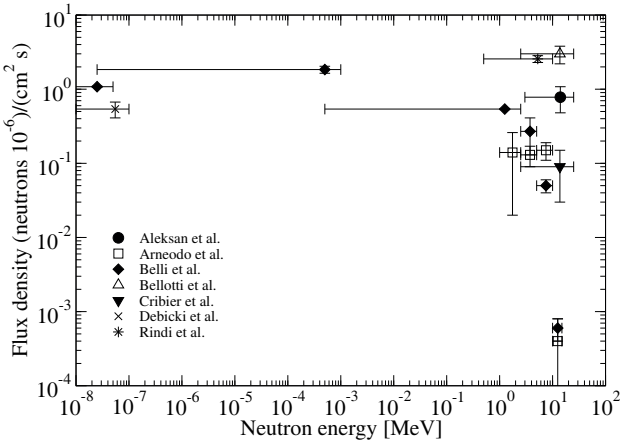

Fig. 5. Comparison of different neutron flux measurements at LNGS.

Reaction studies involving detection of neutrons can also be greatly improved upon in underground laboratories. The background neutron flux at LNGS is typically 2–3 orders of magnitude lower than at a surface laboratory, because of the already reduced flux of neutrons from cosmic-ray muons [72]. Thus, the dominant source of neutrons in underground laboratories arises from (α, n) reactions on light elements ($A \simeq 12$–28) initiated by α-particles from primordial decay chains, mainly of ^{238}U. Since these reactions take place in the rocks and concrete walls of the experimental halls, the measured neutron flux may vary significantly at different locations in the same laboratory. Partial shielding from such neutrons can be obtained by surrounding the experimental setup with a 1m-thick concrete wall, as foreseen at LUNA MV. Figure 5 [74] shows a compilation of neutron flux measurements at LNGS, using data from refs. [75–80]. A more recent measurement [81] of thermal neutron fluxes reported a value of $0.32 \pm 0.09(\text{stat.}) \pm 0.02(\text{sys.})[10^{-6}\,\text{cm}^{-2}\,\text{s}^{-1}]$, in good agreement with that of ref. [74]. Possible beam-induced (α, n) background could come from impurities in the target material or along the beam-lines (*e.g.* slits, collimators), mostly from ^{11}B(α, n) [50] and ^{17,18}O(α, n) reactions [50, 82]. If the neutron detector is also sensitive to γ-rays, one should also consider possible (n, γ) and (α, γ) reactions.

Unlike charged particles and gamma rays, neutrons do not interact directly with electrons in matter. Their detection is thus based on indirect methods, such as (in)elastic scattering by a light nucleus (hydrogen or helium) or induced nuclear reactions, leaving the products of these reactions to initiate the detection process. Reaction-based counters (such as ^{3}He or BF_3 tubes) take advantage of the increased reaction probability at low neutron energy by moderating the incoming neutrons, but knowledge of the initial neutron energy before moderation is lost. Thus, in general, neutron detectors provide information only on the number of neutrons detected and not on their energy.

For the two neutron source reactions, ^{13}C$(\alpha, n)^{16}$O and ^{22}Ne$(\alpha, n)^{25}$Mg, ^{3}He counters have traditionally been used [50, 53, 68], embedded within a polyethylene cylinder moderator in a 4π geometry with overall efficiency of up to 50%. In one case [68], some information on the neutron energy was extracted from the count ratio between inner and outer ring tubes. However, the intrinsic activity[1] of ^{3}He counters may be a limiting factor for low-rate neutron detection underground. Alternative approaches may include the use of compact γ-ray arrays coupled with an (n, γ) converter, albeit with a much reduced efficiency (*e.g.* 10–25% in [83]). Thus, a new design for optimal neutron detection underground is required.

Suitable alternatives to traditional neutron counters may come from Li-loaded glasses, among the most popular inorganic scintillators. Cerium-activated ^{6}Li-glass scintillators have proven to be a powerful tool in the study of neutrons in the keV range. The detection process is based on the ^{6}Li$(n, \alpha)^3$H reaction ($Q = 4.8\,\text{MeV}$), whose cross section for thermal neutrons ($E_\text{n} < 0.5\,\text{eV}$) is 945 barn. An alternative to ^{6}Li glass detectors is provided by flat detection screens consisting in a thin layer of zinc sulphide phosphor (ZnS:Ag)[2] scintillator loaded with ^{6}LiF. Such sheets are available in different sizes and typical thicknesses of 0.3–0.5 mm (EJ-426 by Eljen Technology [84]), thus allowing for very compact geometries. The efficiency of ^{6}Li glass scintillators depends on both detector type and thickness and in some cases efficiencies as high as 80–100% have been reported [85], with little γ-ray sensitivity.

A further alternative to the detectors considered so far would be the use of liquid scintillators (*e.g.* BC501 [86] or ^{10}B-loaded BC523 [87]) to allow for discrimination between fast neutrons and gamma rays. Tests with ^{252}Cf and AmBe sources have led to efficiencies of about 50% for $E_n = 0.5$–$5\,\text{MeV}$ for a $5'' \times 5''$ cylindrical BC501 scintillator [88]. Clearly, a major concern for the best choice will be the evaluation of the detector's intrinsic activity as measured underground. Test measurements with some prototypes are expected to take place in the coming months. Options to inform the best choice of neutron detection underground are currently being considered.

4 Conclusion

The key reactions of the He-burning phase, ^{12}C$(\alpha, \gamma)^{16}$O, ^{13}C$(\alpha, n)^{16}$O, ^{22}Ne$(\alpha, n)^{25}$Mg, play an outstanding role in stellar evolution and nucleosynthesis. The ^{12}C$(\alpha, \gamma)^{16}$O is known as the "Holy Grail" of nuclear astrophysics. It determines the production of C and O, elements of primary importance in biological processes. The ultimate fate of all the stars, from the massive ones, which end their life with a core collapse, to those of small and intermediate mass, which evolve into white dwarfs and may originate violent phenomena powered by thermonuclear explosions, such as

[1] The internal background of ^{3}He counters is mainly due to alpha emitters of the uranium and thorium series present as trace elements in the construction material of the tubes. In surface laboratories this background is not directly observable, since completely masked by the cosmic-ray–induced background.

[2] The specific attraction of zincsulphide (ZnS) is that its gamma sensitivity is low.

novae and supernovae of type Ia, depends on the C/O ratio left by the He burning. Finally, the last two reactions are the most important sources of neutrons in stars and allow the activation of a fundamental nucleosynthesis process (the *s*-process). About half of the elements heavier than iron are synthesized through the s process. As a whole, the cross sections of these and other reactions are important input for understanding the evolution of stars, their nucleosynthesis and the properties of the stellar plasma.

Efforts to measure the cross sections of the above mentioned reactions at the relevant astrophysical energies have been lasting worldwide for decades but the experimental problem is still open. An opportunity to fix these tiles of the nuclear astrophysics mosaic comes with the next-generation deep underground accelerator facilities, where the abatement of cosmic ray background can make measureable the expected feeble counting rates. New underground facilities are under construction in Italy (Gran Sasso National Laboratory: beam energy = 3.5 MeV) [73], USA-SD (Homestake mine: beam energy = 1 MeV) [89] and in China (Jinping Laboratory: beam energy = 0.4 MeV) [89]. The underground deployment of the next experiments will be not enough to reach the goal: developments of new solid and/or gas targets resilient to intense alpha beams and of high-efficiency detectors with large angular coverage and, in the case of γ detection, high granularity are also definitively needed as well as extremely challenging.

Finally, the next-generation underground experiments can really mark a step forward in making true the famous William Fowlers statement: "It is a remarkable fact that humans, on the basis of experiments and measurements carried out in the lab, are able to understand the universe".

References

1. F. Hoyle, D.N.F. Dumbar, W.A. Wensel, W. Whaling, Phys. Rev. **92**, 649 (1953).
2. P.G. Prada Moroni, O. Straniero, Astroph. J. **581**, 585 (2002).
3. A. Burrows, Rev. Mod. Phys. **85**, 245 (2013).
4. G. Imbriani *et al.*, Astroph. J. **558**, 903 (2001).
5. I. Domínguez, P. Höflich, O. Straniero, Astroph. J. **557**, 279 (2001).
6. C. Angulo *et al.*, Nucl. Phys. A **656**, 3 (1999).
7. R. Kunz, M. Jaeger, A. Mayer, J.W. Hammer *et al.*, Phys. Rev. Lett. **86**, 3244 (2001).
8. O. Straniero, I. Domínguez, G. Imbriani, L. Piersanti, Astroph. J. **583**, 878 (2003).
9. O. Straniero, R. Gallino, S. Cristallo, Nucl. Phys. A **777**, 311 (2006).
10. R. Gallino *et al.*, Astroph. J. **497**, 388 (1998).
11. F. Kaeppeler *et al.*, Astroph. J. **437**, 396 (1994).
12. L.R. Yungelson, *White Dwarfs: Cosmological and Galactic Probes*, edited by E.M. Sion, S. Vennes, H.L. Shipman, in *Astrophys. Space Sci. Lib.*, Vol. **332** (Springer, Berlin, 2005) pp. 163–173.
13. P. Hoeflich, A. Khokhlov, Astroph. J. **457**, 500 (1996).
14. P.G. Prada Moroni, O. Straniero, Astron. Astrophys. **466**, 1043 (2007).
15. J.D. Larson, R.H. Spears, Nucl. Phys. A **56**, 497 (1964).
16. P. Dyer, C.A. Barnes, Nucl. Phys. A **233**, 495 (1974).
17. K.U. Kettner, H.W. Becker, L. Buchmann, J. Görres, *et al.*, Z. Phys. A **308**, 73 (1982).
18. A. Redder, H.W. Becker, C. Rolfs, H.P. Trautvetter *et al.*, Nucl. Phys. A **462**, 385 (1987).
19. R.M. Kremer, C.A. Barnes, K.H. Chang, H.C. Evans, B.W. Filippone, Phys. Rev. Lett. **60**, 1475 (1988).
20. J.M.L. Ouellet, M.N. Butler, H.C. Evans, H.W. Lee *et al.*, Phys. Rev. C **54**, 1982 (1996).
21. G. Roters, C. Rolfs, F. Strieder, H.P. Trautvetter, Eur. Phys. J. A **6**, 451 (1999).
22. L. Gialanella, D. Rogalla, F. Strieder, S. Theis *et al.*, Eur. Phys. J. A **11**, 357 (2001).
23. M. Fey, PhD thesis, Universität Stuttgart, Germany (2004).
24. M. Assunção, M. Fey, A. Lefebvre-Schuhl, J. Kiener *et al.*, Phys. Rev. C **73**, 055801 (2006).
25. C. Matei, L. Buchmann, W.R. Hannes, D.A. Hutcheon *et al.*, Phys. Rev. Lett. **97**, 242503 (2006).
26. H. Makii *et al.*, Phys. Rev. C **80**, 065802 (2009).
27. D. Schürmann *et al.*, Phys. Lett. B **703**, 557 (2011).
28. R. Plag *et al.*, Phys. Rev. C **86**, 015805 (2012).
29. M. D'Agostino Bruno *et al.*, Nuovo Cimento A **27**, 1 (1975).
30. R. Plaga *et al.*, Nucl. Phys. A **465**, 291 (1987).
31. P. Tischhauser, R.E. Azuma, L. Buchmann, R. Detwiler *et al.*, Phys. Rev. Lett. **88**, 072501 (2002).
32. P. Tischhauser, A. Couture, R. Detwiler, J. Görres *et al.*, Phys. Rev. C **79**, 055803 (2009).
33. Z. Zhao *et al.*, Phys. Rev. Lett. **70**, 2066 (1993).
34. R.E. Azuma, L. Buchmann, F.C. Barker, C.A. Barnes *et al.*, Phys. Rev. C **50**, 1194 (1994).
35. R.H. France, III, E.L. Wilds, J.E. McDonald, M. Gai, Phys. Rev. C **75**, 065802 (2007).
36. X.D. Tang, K.E. Rehm, I. Ahmad, C.R. Brune *et al.*, Phys. Rev. Lett. **99**, 052502 (2007).
37. C.R. Brune, W.H. Geist, R.W. Kavanagh, K.D. Veal, Phys. Rev. Lett. **83**, 4025 (1999).
38. S. Adhikari, C. Basu, Phys. Lett. B **704**, 308 (2011).
39. M.L. Avila *et al.*, Phys. Rev. Lett. **114**, 071101 (2015).
40. D. Schürmann, A. Di Leva, L. Gialanella, D. Rogalla *et al.*, Eur. Phys. J. A **26**, 301 (2005).
41. C.R. Brune, Phys. Rev. C **66**, 044611 (2002).
42. A.M. Lane, R.G. Thomas, Rev. Mod. Phys. **30**, 257 (1958).
43. F.C. Barker, T. Kajino, Aust. J. Phys. **44**, 369 (1991).
44. D. Schrmann, L. Gialanella, R. Kunz, F. Strieder, Phys. Lett. B **711**, 35 (2012).
45. M. Gai, Phys. Rev. C **88**, 062801 (2013).
46. O. Straniero, S. Cristallo, L. Piersanti, Astropyis. J. **785**, 77 (2014) arXiv:1403.0819 [astro-ph.GA].
47. M. Heil *et al.*, Phys. Rev. C **78**, 025803 (2008).
48. O. Straniero, R. Gallino, S. Cristallo, Nucl. Phys. A **777**, 311 (2006) Special Issue on *Nuclear Astrophysics*.
49. S. Cristallo *et al.*, Astrophys. J. **696**, 797 (2009).
50. H.W. Drotleff *et al.*, Astrophys. J. **414**, 735 (1993).
51. C.R. Brune, I. Licot, R.W. Kavanagh, Phys. Rev. C **48**, 3119 (1993).
52. C.N. Davids, Nucl. Phys. A **110**, 619 (1968).
53. S. Harissopulos *et al.*, Phys. Rev. C **72**, 062801 (2005).
54. P. Descouvemont, Phys. Rev. C **36**, 2206 (1987).
55. B. Guo *et al.*, Astrophys. J. **756**, 193 (2012).
56. S. Kubono *et al.*, Phys. Rev. Lett. **90**, 062501 (2003).

57. N. Keeley, K. Kemper, D.T. Khoa, Nucl. Phys. A **726**, 159 (2003).
58. M.G. Pellegriti *et al.*, Phys. Rev. C **77**, 042801 (2008).
59. E.D. Johnson *et al.*, Phys. Rev. Lett. **97**, 192701 (2006).
60. M.L. Avila *et al.*, Phys. Rev. C **91**, 048801 (2015).
61. M. La Cognata *et al.*, Phys. Rev. Lett. **109**, 232701 (2012).
62. C. Ugalde, PoS **(NIC X)**, 038 (2008).
63. M. Jaeger *et al.*, Phys. Rev. Lett. **87**, 202501 (2001).
64. R. Longland, C. Iliadis, A.I. Karakas, Phys. Rev. C **85**, 065809 (2012).
65. U. Giesen *et al.*, Nucl. Phys. A **561**, 95 (1993).
66. R. Longland *et al.*, Phys. Rev. C **80**, 055803 (2009).
67. C.E. Porter, R.G. Thomas, Phys. Rev. **104**, 483 (1956).
68. M. Jaeger *et al.*, Phys. Rev. Lett. **87**, 202501 (2001).
69. C. Rolfs, W. Rodney, *Cauldrons in the Cosmos* (University of Chicago Press, Chicago, 1988).
70. H. Costantini *et al.*, Rep. Prog. Phys. **72**, 086301 (2009).
71. R. Longland, C. Iliadis, A. Champagne, C. Fox, J. Newton, Nucl. Instrum. Methods Phys. Res. **566**, 452 (2006).
72. A. Best *et al.*, Eur. Phys. J. A **52**, 72 (2016) contribution to this Topical Issue.
73. A. Guglielmetti, Phys. Dark Univ. **4**, 10 (2014).
74. Z. Dębicki *et al.*, Nucl. Phys. B Proc. Suppl. **196**, 429 (2009).
75. E. Bellotti, Report INFN/TC-85/19 Istituto Nazionale Fisica Nucleare (1985).
76. A. Rindi, F. Celani, M. Lindozzi, S. Miozzi, Nucl. Instrum. Methods Phys. Res. A **272**, 871 (1988).
77. P. Belli *et al.*, Nuovo Cimento A **101**, 959 (1989).
78. R. Aleksan *et al.*, Nucl. Instrum. Methods Phys. Res. A **274**, 203 (1989).
79. M. Cribier *et al.*, Astropart. Phys. **4**, 23 (1995).
80. F. Arneodo *et al.*, Nuovo Cimento A **112**, 819 (1999).
81. A. Best *et al.*, Nucl. Instrum. Methods A **812**, 1 (2016).
82. S. Falahat, PhD thesis, University of Mainz (2010).
83. M. Heil *et al.*, Phys. Rev. C **78**, 025803 (2008).
84. `http://www.eljentechnology.com`.
85. `http://www.detectors.saint-gobain.com`.
86. `http://www.crystals.saint-gobain.com/uploadedFiles/SG-Crystals/Documents/SGC%20BC501_501A_519%20Data%20Sheet.pdf`.
87. `http://www.crystals.saint-gobain.com/uploadedFiles/SG-Crystals/Documents/SGC%20BC523A%20Data%20Sheet.pdf`.
88. G. Ciani, *Rivelazione di neutroni in esperimenti di astrofisica nucleare: studio e caratterizzazione di scintillatori liquidi organici*, Master's thesis, Università di Bari (2015).
89. W.-P. Liu, Z.-H. Li, Y.-B. Wang, B. Guo, Y.-P. Shen (Editors), *Proceedings of The 13th International Symposium on Origin of Matter and Evolution of Galaxies (OMEG2015) Beijing, China, June 24-27, 2015*, in *EPJ Web of Conferences*, Vol. **109** (2016).